MICROSTRUCTURES AND TEXTURE OF INCONEL 718 ALLOY FABRICATED BY SELECTIVE LASER MELTING

LI SHUAI, WEI QINGSONG(*CORRESPONDING AUTHOR*)
State key Lab of Materials Processing and Die&Mould Technology, School of Materials Science and Engineering, Huazhong University of Science and Technology
No1037 Luoyu Road, Hongshan District, Wuhan 430074, China

ZHANG DQ, CHUA CHEE KAI (CHUA C. K.)
NTU Additive Manufacture Centre, Nanyang Technological University,
50 Nanyang Avenue, Singapore 639798

ABSTRACT: Inconel 718 nick base superalloy samples were fabricated by selective laser melting from the powder. The microstructure examinations reveal that fine cellular and dendritic structures with a size smaller than 1μm were formed in the laser track due to the rapid cooling speed. In order to investigate the influence of the anisotropy, two scanning strategies were used namely bidirectional and rotate 90˚ between neighboring layers in this study. The Inverse Polar Figure (IPF) acquired by electron backscatter diffraction (EBSD) proves that both of them show strong texture long the building directional. However, the texture can be significantly reduced by adjusting the scanning strategies.

Keywords: Additive manufacturing; Selective laser melting; nickel based superalloy; Microstructure; texture.

1. Introduction

Selective Laser Melting (SLM) based on additive manufacturing (AM) principles, uses the laser with a high energy density (such as ytterbium fiber laser) to create 3D metal parts by melting continuous thin layers of metallic powders(Chua, Leong et al. 2010, Gu and Zhang 2013, Liu, Zhang et al. 2013, Loh, L., et al. 2014, Papadakis, Loizou et al. 2013). It is a promising technology for manufacturing metal parts with complex and fine geometries.

Nickel base alloys were used widely in aerospace, nuclear and automobile industries due to their good corrosion resistance, high temperature strength and fine thermal expansion. Recently, many researchers have focused on SLM processing of nickel base alloys such as Inconel 718(Amato, Gaytan et al. 2012, Wang, Guan et al. 2012), Inconel 625(Yadroitsev, Thivillon et al. 2007), Nimonic 263(Vilaro, Colin et al. 2012) and NI 738LC(Rickenbacher, Etter et al. 2013). The microstructures of all the above materials have been investigated using different methods, in which fine cellular grains were obtained due to the rapid cooling speed during SLM process. Some researchers (Amato, Gaytan et al. 2012, Vilaro, Colin et al. 2012, Rickenbacher, Etter et al. 2013, Song, Dong et al. 2014)found that the as-SLM samples exhibited high yield and ultimate strengths that were higher or close to those of wrought samples. Although the SLM parts presented good mechanical properties, they also showed a strong anisotropy due to the directional columnar grain growth caused by directional thermal conduction during SLM process. High ductility could be obtained when the grains orientations were parallel to the tensile load direction(Song, Dong et al. 2014), whereas low ductility but high yield and ultimate tensile strengths could be found as the grain orientation was vertical to the tensile load direction (Thijs, Montero Sistiaga et al. 2013). The

Proc. of the Intl. Conf. on Progress in Additive Manufacturing
Edited by Chua Chee Kai, Yeong Wai Yee, Tan Ming Jen and Liu Erjia

ISBN: 978-981-09-0446-3 :: doi:10.3850/978-981-09-0446-3_021

grain orientation depends on the texture in the sample. The texture has significant influence on the mechanical properties. Unfortunately, there are few literatures give a deep analysis about the texture so far(Niendorf, Leuders et al. 2013).
Therefore, this study investigated the of as-SLM fabricated Inconel 718 superalloy samples; the grain structures of horizontal and vertical sections were observed by scanning electron microscope (SEM); the influences of the scanning strategy of laser beam on the texture were characterized by electron backscatter diffraction (EBSD); and the explanation was given to addressed the formation of the microstructure and the texture of Inconel 718 alloy produced by SLM.

2. Materials and experimental

2.1 Produced of the samples

A commercials Inconel 718 powder (H.C. Starck GmbH, Germany) produced by gas atomized process with the average particle size of 34.63μm was used. The shape is approximately spherical and the surface is smooth. The chemical composition was of 55.0 Ni, 17.85 Cr, 17.33 Fe, 0.85 Ti, 2.86 Mo, 0.57Al, 0.29 Co in wt%. Figure 1(a) illustrates the SEM morphology of the powder .The powder was pre-heated at 50˚C for 5 hours in the furnace before SLM to eliminate the water vapor on the surface of the powder.. The SLM testings were conducted on the HRPM-II machine that was developed by Huazhong University of Science and Technology. The processing chamber was vacuumed and then filled with argon gas, preventing possible materials oxidation during SLM process.
The optimized processing parameters obtained by our group were adopted for manufacturing of almost fully dense Inconel 718 parts, which are the laser power of 160W, the scan speed of 500mm/s, the hatch space of 0.06mm, and the layer thickness of 0.02mm. In order to investigate the influence of the laser scanning path on the texture, two scanning strategies, namely bidirectional and rotate 90˚ between neighboring layers were used, as shown in figure 1b. The samples produced by those two scanning strategies were named Bi-samples and Ro-samples respectively.

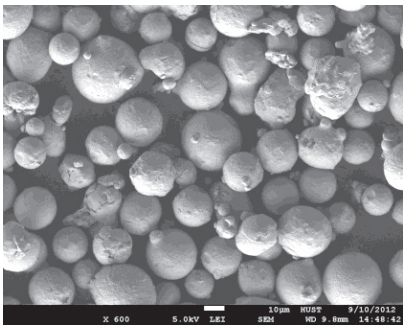

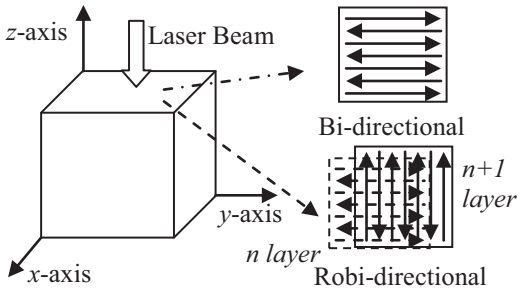

Figure 1. (a) SEM morphology of the Inconel 718 powder. (b) Schematic diagram of the laser scanning strategies.

2.2 Microstructures and texture characterizations

The Bi-samples were polished using a grit size of 1 μm in both horizontal (*xy)* and vertical (*xz)* sections. Subsequently, the polished samples were etched for 30s in a mixture comprising solution with 10ml HNO_3, 10ml HCL and 15ml CH_3COOH.
The vertical (*xz)* sections of both Bi-samples and Ro-samples were mechanically polished firstly, and then employed by electrochemical polishing to eliminate the residual stresses come from SLM and mechanical polishing processes. EBSD was measured using a HKL Nordlys S electron

backscatter diffraction system equipped on a field emission gun SEM machine. The step sizes for the measurements were 1 μm. The data was analyzed using HKL Channel 5 software program.

3 Results and Discussions

3.1 Morphologies of melted pools and grains

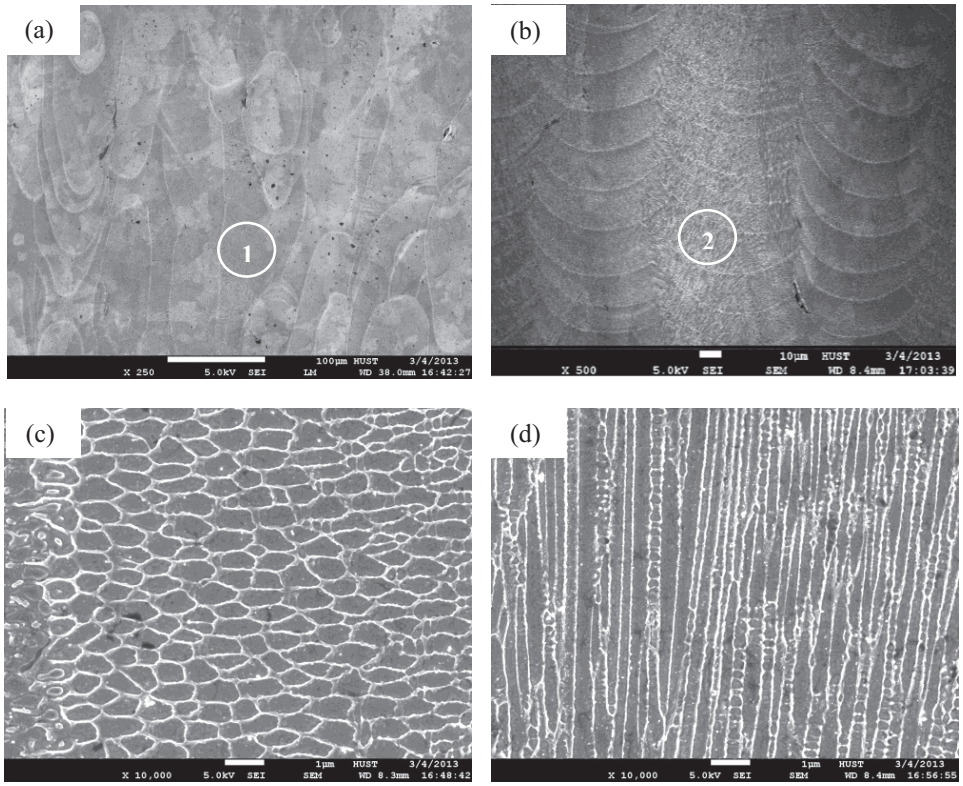

Figure 2. SEM morphologies of the melted pools and grains of Bi-samples. The images of horizontal (xy) and vertical (xz) sections were shown in (a) and (b) respectively. Two typical microstructures, cellular and dendritic structures, were found in area 1 and 2, as shown in (c) and (d) at the high-magnification respectively.

Fig.2 shows the microstructures of the Bi-samples. The melted pools corresponding to the laser tracks can be seen clearly. A single track can be recognized as the foundation of the SLM produced parts. Multi-line and multi-layer of single tracks were accumulated to form a 3d object. Base on the pixel count, the height of the neighboring layer is approximately 30μm which is not exactly coinciding with the layer thickness (0.02mm). It may be the result of shrinkage of loose powder during SLM process. The real layer thickness H_r can be calculated according to the equation (Cai, Liu et al. 2010):

$$H_r=h_s\rho_r/\rho_p \quad (1),$$

where, h_s is the thickness parameter that set for the SLM process. ρ_r is the density of the solid material. ρ_p is the apparent density of the powder. In this study, h_s is 20μm and ρ_r/ρ_p is approximately 1.8 according to literatures (Khan and Dickens 2010). And then, H_r is 36μm which is agree with the measurement.

In addition, fine cellular and dendritic structures with a size less than 1μm were found within every laser tracks. The internal of the grain is made up of nickel base, and the boundary is mainly composed by Nb, Ti and Mo elements(Dinda, Dasgupta et al. 2012). Inconel 718 is an ageing strengthening superalloy and the obtain its maximum strength from coherently ordered body-centered tetragonal γ" (Ni_3Nb) and face centered cubic γ' ($Ni_3(Al,Ti)$) precipitates. Due to these strengthen elements get together along the cellular boundaries, it may be hard to form precipitated phases. Therefore, no precipitation is observed by the SEM. The average cellular size is about 1μm based on the pixel count in Figure 2c, which is approximately two orders of magnitude lower than that of the traditional castings (100-300μm). Therefore, it is easy to eliminate the element segregation of the SLM samples due to those fine grains through post heat treatments (Mehrabian 1982), and then to obtain good mechanical properties such as hardness and room temperature tensile properties.

3.2 The texture of the SLM parts

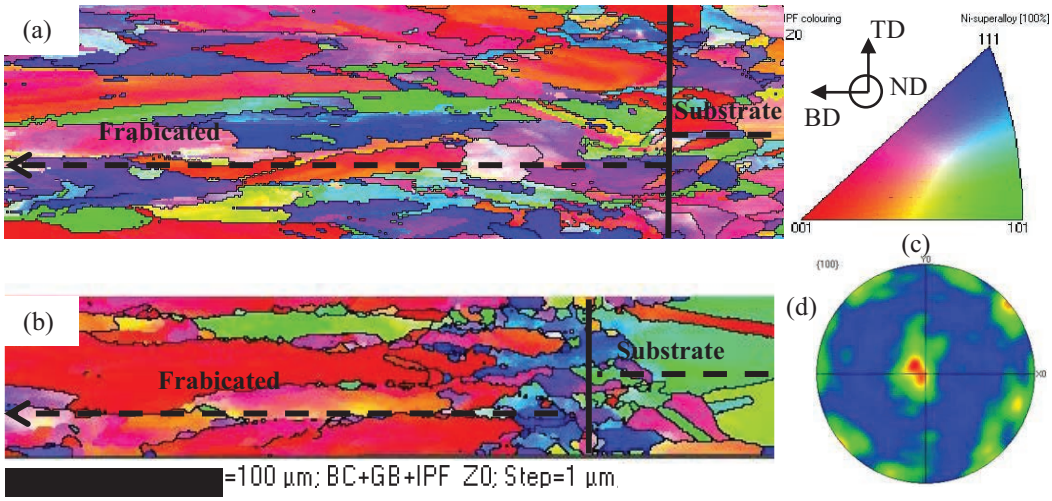

Figure 3. EBSD orientation maps of the vertical (xz) sections of as-SLM samples including the substrates. The building direction is indicated by the black arrows: (a) Inverse Pole Figure (IPF) of the Bi-samples. (b) IPF of the Ro-samples. (c) The index map of the IPF and the reference coordinate (d) (100) pole figure of the IPF image of the Bi-sample

Figures 3a and 3b show the IPF of the Bi- and Ro-samples respectively. In IPF maps, a grain boundary is defined if the misorientation angle between the neighboring colors is over 20˚. Hence, some larger elongation grains of several hundred micrometers in length grow cross a few layers. A very strong texture can be identified for the SLM sample. The growth direction of the grain mainly depended on the thermal conduction and the fastest growth direction. In SLM process, thermal gradient generates from the top layer to the substrate or the solidified layer and the grain, and tends to grow along the direction of heat flow. In initial several layers that are close to the substrate, the

grains inherit the growth directions of the substrate. It is known that for inconel alloy the preferential growth direction is <100>(Dinda, Dasgupta et al. 2012). Therefore, the <100> direction become the major growth direction of the grains after several layers, which has been confirmed by the IPF maps in Figure 3 Comparison of figures 3a and 3b indicates that the laser scanning strategy has a significant influence on the texture of the as-SLM fabricated parts. The bidirectional scanning strategy greatly reduced the degree of texture, and a weak cubic texture was formed as shown in figure 3d.

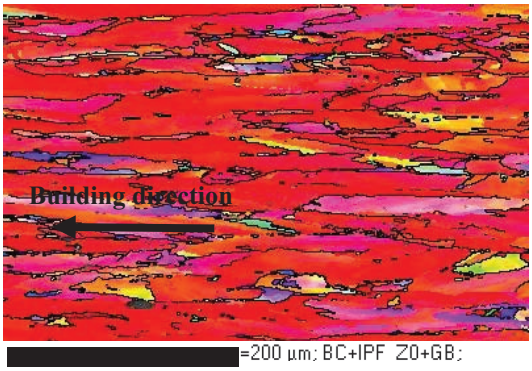

Figure 4. The IPF map of the vertical (xz) section that is approximately 5 mm far from the substrate of the Ro-samples

Figure 4 shows the orientation of the grains in the region that is far from the substrate of the Ro-samples. The texture degree is higher than that of the processing beginning. Almost all of the grains grow along the <100> direction, corresponding to the adding direction of layers. The temperature of the melted pool is not uniform due to the Gaussian energy distribution of laser beam, which causes that the convection within every melted pool cannot be completely eliminated (Dai and Gu 2014). That internal convection of heat flow results in different grain growth directions, which can be confirmed by a small number of regions in figure 4. However, the significant texture can be obtained along the vertical direction during SLM of Inconel 718 alloy from a general view. These studies in texture can provide good evidences for the anisotropic of the SLM produced parts.

3 Conclusions

(1) SEM morphologies of multi-line and multi-layer melted pools and the grains within every melted pool on horizontal and vertical sections were characterized for the Inconel 718 alloy produced by SLM. Fine cellular and dendritic structures with a size less than 1 μm were observed.
(2) EBSD detections indicate that a significant texture is formed along the vertical direction during SLM of Inconel 718 alloy due to the directional thermal conduction. The IPF maps show that most of grains grow along the <100> direction. This trend increases with the increasing of manufacturing height. However, the degree of texture would be influenced by the laser scanning strategies; it may be adjusted by using different laser scanning strategies.

ACKNOWLEDGMENTS
The authors acknowledge the financial supports from the National Natural Science Foundation of China (NSFC, Grant No: 51375189 and No. 51375188), the National Science & Technology Pillar

Program of China (Granted No 2012BAF08B00), the ministry of education innovation team development project (IRT1244). The study was also co-funded by China Scholarship Council (CSC).

REFERENCES

Amato, K., et al. (2012). Microstructures and mechanical behavior of Inconel 718 fabricated by selective laser melting. *Acta materialia* 60(5): 2229-2239.

Chua, C. K., et al. (2010). *Rapid prototyping: principles and applications*, World Scientific.

Dai, D. and D. Gu (2014). "Thermal behavior and densification mechanism during selective laser melting of copper matrix composites: Simulation and experiments." *Materials & Design* 55: 482-491.

Dinda, G., et al. (2012). "Texture control during laser deposition of nickel-based superalloy." *Scripta Materialia* 67(5): 503-506.

Gu, D. and G. Zhang (2013). "Selective laser melting of novel nanocomposites parts with enhanced tribological performance: " *Virtual and Physical Prototyping* 8(1): 11-18.

Khan, M. and P. Dickens (2010). "Selective Laser Melting (SLM) of pure gold." *Gold Bulletin* 43(2): 114-121.

Liu, Z., et al. (2013). "Crystal structure analysis of M2 high speed steel parts produced by selective laser melting." *Materials Characterization* 84: 72-80.

Loh, L., et al. (2014). "Selective Laser Melting of aluminium alloy using a uniform beam profile: The paper analyzes the results of laser scanning in Selective Laser Melting using a uniform laser beam." *Virtual and Physical Prototyping* **9**(1): 11-16.

Mehrabian, R. (1982). "*Rapid solidification.*" International Materials Reviews 27(1): 185-208.

Niendorf, T., et al. (2013). "Highly Anisotropic Steel Processed by Selective Laser Melting." *Metallurgical and Materials Transactions B:* 1-3.

Papadakis, L., et al. (2013). "A computational reduction model for appraising structural effects in selective laser melting manufacturing." *Virtual and Physical Prototyping(ahead-of-print)*: 1-9.

Rickenbacher, L., et al. (2013). "High temperature material properties of IN738LC processed by selective laser melting (SLM) technology." *Rapid Prototyping Journal* 19(4): 282-290.

Song, B., et al. (2014). "Fabrication of NiCr alloy parts by selective laser melting: columnar microstructure and anisotropic mechanical behavior." *Materials & Design* 53: 1-7.

Thijs, L., et al. (2013). "Strong morphological and crystallographic texture and resulting yield strength anisotropy in selective laser melted tantalum." *Acta materialia.*

Vilaro, T., et al. (2012). "Microstructural and mechanical approaches of the selective laser melting process applied to a nickel-base superalloy." *Materials Science and Engineering: A* 534: 446-451.

Wang, Z., et al. (2012). "The microstructure and mechanical properties of deposited-IN718 by selective laser melting." *Journal of Alloys and Compounds* 513: 518-523.

Yadroitsev, I., et al. (2007). "Strategy of manufacturing components with designed internal structure by selective laser melting of metallic powder." *Applied Surface Science* 254(4): 980-983.

Zhang DQ, et al. (2010). "A Powder Shrinkage Model for Describing Real Layer Thickness during Selective Laser Melting Process." *Advanced Materials Research* 97: 3820-3823.